APPLIED SCIENCES AND ENGINEERING

Extracellular polymeric substances are transient media for microbial extracellular electron transfer

Yong Xiao,[1,2] Enhua Zhang,[1,3] Jingdong Zhang,[2] Youfen Dai,[1] Zhaohui Yang,[3] Hans E. M. Christensen,[2] Jens Ulstrup,[2] Feng Zhao[1]*

Microorganisms exploit extracellular electron transfer (EET) in growth and information exchange with external environments or with other cells. Every microbial cell is surrounded by extracellular polymeric substances (EPS). Understanding the roles of three-dimensional (3D) EPS in EET is essential in microbiology and microbial exploitation for mineral bio-respiration, pollutant conversion, and bioenergy production. We have addressed these challenges by comparing pure and EPS-depleted samples of three representative electrochemically active strains viz Gram-negative *Shewanella oneidensis* MR-1, Gram-positive *Bacillus* sp. WS-XY1, and yeast *Pichia stipites* using technology from electrochemistry, spectroscopy, atomic force microscopy, and microbiology. Voltammetry discloses redox signals from cytochromes and flavins in intact MR-1 cells, whereas stronger signals from cytochromes and additional signals from both flavins and cytochromes are found after EPS depletion. Flow cytometry and fluorescence microscopy substantiated by *N*-acetylglucosamine and electron transport system activity data showed less than 1.5% cell damage after EPS extraction. The electrochemical differences between normal and EPS-depleted cells therefore originate from electrochemical species in cell walls and EPS. The 35 ± 15–nm MR-1 EPS layer is also electrochemically active itself, with cytochrome electron transfer rate constants of 0.026 and 0.056 s^{-1} for intact MR-1 and EPS-depleted cells, respectively. This surprisingly small rate difference suggests that molecular redox species at the core of EPS assist EET. The combination of all the data with electron transfer analysis suggests that electron "hopping" is the most likely molecular mechanism for electrochemical electron transfer through EPS.

INTRODUCTION

Electron transfer (ET) is one of the most fundamental life processes, and microorganisms exploit extracellular electron transfer (EET) to exchange information and energy with other microorganisms or with their external environments (*1*–*6*). Two mechanistically overarching EET pathways have been proposed (*2*, *7*–*10*) (Fig. 1A): (i) direct "band-like" electron conductivity, where electrons are transported via extended conductive pili/nanowires or redox proteins located in the microbial outer membrane; and (ii) indirect EET, where ET is mediated by mobile or spatially fixed molecular redox shuttles. However, neither of these pathways has been reported to involve extracellular polymeric substances (EPS).

EPS are fundamental microbial components that determine the physiochemical properties of biofilms (*11*). Almost every microbial cell is surrounded by EPS, which assist in biofilm formation and protection from unfavorable environment (*11*–*13*). Atomic force microscopy (AFM) shows, for example, that *Azospirillum brasilense* forms a 2-nm layer of adsorbed EPS on polystyrene substrata after 24 hours of growth (*14*), whereas cryo-transmission electron microscopy has shown that *Shewanella oneidensis* MR-1 (MR-1) in biofilm is enveloped by an EPS layer up to 1 μm after a 110-day cultivation (*15*). EPS contribute to biogeochemical cycles of organic matter and nutrient elements. Many components of EPS, such as DNA, humic acids, and some proteins, are redox-active or conductive/semiconductive (*16*). Some studies have shown that EPS are able to synthesize metal nanoparticles in the presence of c-type cytochromes (*17*) and have redox properties similar to MR-1 (*18*). However, it is poorly understood whether EPS are directly involved in EET processes, because previous microbial EET studies were only conducted on biofilms with EPS retained or on cells from the log stage or early steady stage cultures with little EPS. Note that electron transport between the cells and extracellular electron acceptors/donors must pass through the layer of EPS, but it is not known whether these electrons would be captured or whether the ET processes are speeded up by the EPS during the process. Hence, it becomes essential to clarify the EPS function in EET via the direct or indirect pathway (Fig. 1B).

With a view on possible mapping of EPS-based EET mechanisms (*16*), we address here the electrochemical behavior of EPS using three electrochemically active strains: Gram-negative MR-1 (*8*), Gram-positive *Bacillus* sp. WS-XY1 (WS-XY1) (*19*), and yeast *Pichia stipitis* (*Ps*) (*19*). Electrochemical analysis of both EPS and whole cells in the presence and absence of EPS was undertaken, followed by morphological and chemical investigations. The results suggest strongly that EPS are crucial in bacterial and yeast EET.

RESULTS

EPS are efficiently removed from MR-1

As a widely studied electrochemically active strain (*2*, *8*), MR-1 was first chosen as the main target to address the role of EPS in EET. The strain was cultured statically in Luria-Bertani broth at 30°C for 48 hours to harvest mature cells and obtain more EPS, and a heat treatment was used to remove EPS (*20*).

The present work shows that heating at 38°C for 30 min removes a 35 ± 15–nm EPS layer from MR-1 cells, compared to those from a control group incubated at 30°C for 30 min with the EPS retained (Fig. 2A and table S1). The AFM shows that the MR-1 cell surface is smooth with very little EPS retained after extraction (Fig. 2, B and C, and fig. S1). The spatial extension of the EPS layer in these studies suggests that redox proteins in the outer membrane in EET have no chance to contact extracellular solid electron acceptors/donors directly.

[1]CAS Key Laboratory of Urban Pollutant Conversion, Institute of Urban Environment, Chinese Academy of Sciences, Xiamen 361021, China. [2]Department of Chemistry, Technical University of Denmark, Kgs. Lyngby 2800, Denmark. [3]Key Laboratory of Environmental Biology and Pollution Control, College of Environmental Science and Engineering, Hunan University, Changsha 410082, China.
*Corresponding author. Email: fzhao@iue.ac.cn

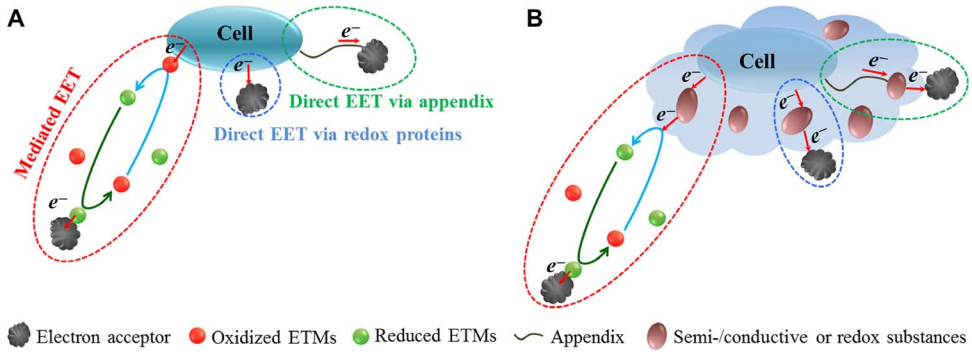

Fig. 1. Representation of microbial EET mechanisms when a microorganism is working as an electron donor. (**A**) A view of previous studies with proposed direct and indirect microbial EET mechanisms. (**B**) Can EET processes be affected when EPS cover the cell surface? ETMs, electron transfer mediators.

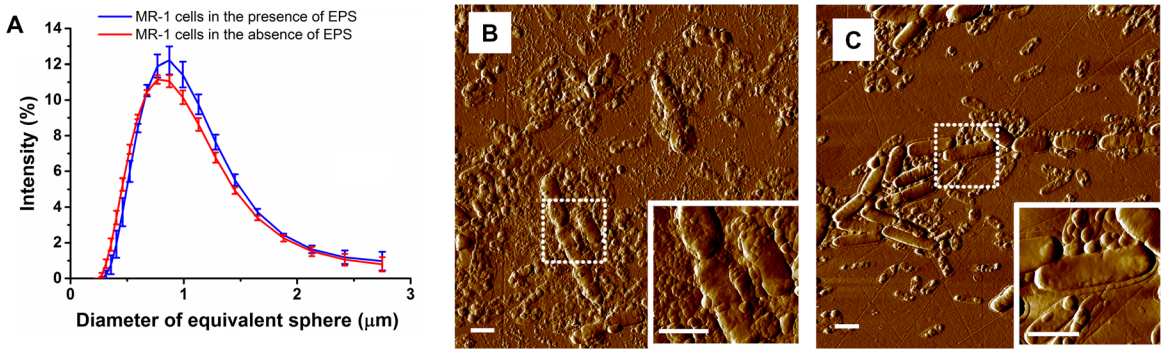

Fig. 2. EPS efficiently removed from MR-1 cells. (**A**) Sphere determination shows a size decrease in MR-1 cells after EPS extraction. (**B**) AFM image showing that MR-1 cells in the control group are enveloped by EPS. (**C**) AFM image showing a smooth MR-1 cell surface after EPS extraction. The insets in (B) and (C) enlarge the dashed boxes. Scale bars in (B) and (C), 2 μm.

EPS from MR-1 are mainly composed of polysaccharides and proteins. Six times more polysaccharide and nine times more protein were detected in EPS extracts from heat-treated MR-1 than from the control group (fig. S2). This accords with a decrease in cell size after EPS extraction (Fig. 2A), a smooth cell surface of EPS-depleted MR-1, and less EPS found after EPS extraction (Fig. 2, B and C).

Electrochemistry of pure and EPS-depleted MR-1 investigated using voltammetry

Cyclic voltammetry (CV) shows barely any difference between the electrochemical signals of pure and EPS-depleted MR-1 (fig. S3). More sensitive differential pulse voltammetry (DPV) was used instead.

MR-1 with EPS retained showed two pairs of DPV peaks (Fig. 3A). The pair with the peak potentials, Ep = −450 mV (anodic, versus Ag/AgCl, unless otherwise stated) and −416 mV (cathodic) are attributed to flavins (*8*, *21*), and the pair at Ep = −138 mV (anodic) and −170 mV (cathodic) attributed to outer membrane c-type cytochromes (*21*, *22*). In the absence of EPS, MR-1 gave two new pairs of DPV peaks with anodic peaks at Ep = −306 and −102 mV and cathodic peaks at *Ep* = −302 and −182 mV, that is, the two flavin peaks have disappeared and an additional pair around −300 mV appeared. These peaks are very similar to those of the flavin/MtrC combination (*21*). EPS removal has thus exposed this combination to the extracellular environment and made the flavin/MtrC interaction detectable. This observation indicates that the flavins are associated with EPS on the cell surface and that the extraction process removes both EPS and diffusing flavins. This suggestion is further verified by DPV on extracted EPS with peaks at −456 and −422 mV (Fig. 3B) and an ultraviolet–visible spectroscopy (UV-vis) absorbance peak at 267 nm (fig. S4A). The two peaks at −182 and −102 mV attributed to c-type cytochromes are retained after EPS extraction, but EPS depletion has enhanced the anodic and cathodic c-type cytochrome peak currents from 28 ± 8 to 38 ± 4 nA and from 84 ± 17 to 113 ± 19 nA, respectively. The enhanced currents indicate that EPS extraction causes more c-type cytochromes to interact with the electrode and facilitate EET. EPS extracts also contain cytochromes, as disclosed by DPV peaks at −153 and −122 mV (Fig. 3B) and a UV-vis absorbance peak at 410 nm (fig. S4B) (*23*).

DPV peaks originate from electrochemically active substances of the cells at the electrode surface. Chronoamperometry was used to address further the origin of the signals. The results show that MR-1 biofilms on glassy carbon electrodes formed in the presence and absence of EPS yield increased currents after lactate addition (fig. S5), indicating that MR-1 cells are active and that the DPV peaks originate from living cells. When lactate was added at the same time point, the maximum current increments from EPS-depleted MR-1 were 40 to 90% higher than that of the control group (table S2), showing that MR-1 in the absence of EPS can transport electrons to extracellular electron acceptors more efficiently than in the presence of EPS. These results accord with the enhanced DPV currents.

MR-1 cells are robust to EPS extraction

To check whether the electrochemical differences between EPS-removed and EPS-retained MR-1 cells originate from leached intercellular substances during the EPS extraction process, we investigated the morphology,

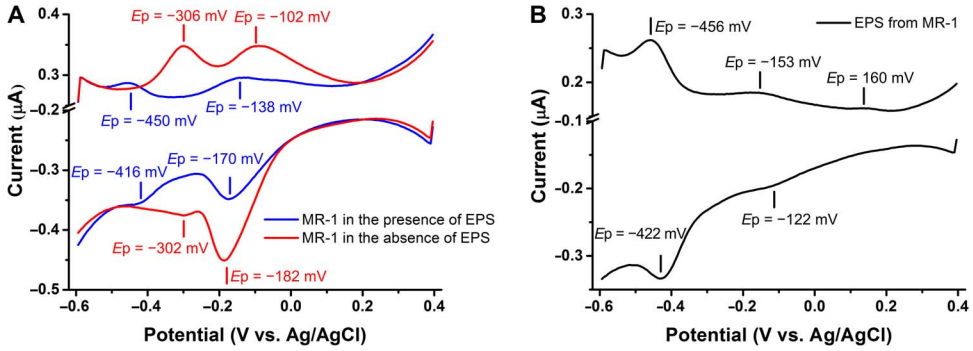

Fig. 3. Electrochemical analysis of MR-1 cells and their EPS. (**A**) DPV of MR-1 cells in the presence of EPS treated at 30°C (blue line) and absence of EPS treated at 38°C (red line). (**B**) DPV of EPS extracted from MR-1 by heating at 38°C.

viability, and activity of MR-1 to verify that the different cell electrochemistry is not caused by cell damage during EPS extraction. Flow cytometry showed that no more than 1.5% of the cells were damaged after EPS extraction (Fig. 4, A and B). This result accords with fluorescence microscopy data using the LIVE/DEAD staining method (Fig. 4, C and D) (*24*). *N*-acetylglucosamine (NAG), one of the monomers of peptidoglycan in bacterial cell walls, is released when cell walls are damaged (*25*). NAG in EPS extract was therefore used to examine the possible damage to MR-1 (Fig. 4E). NAG in EPS extracted at 30° or 38°C was found at similar levels of less than 14 mg/(g dry cell). On the other hand, when MR-1 was treated at 100°C, which destroyed most of the bacterial cells, up to 39 mg/(g dry cell) of NAG was detected in EPS, confirming that 38°C heat treatment causes only insignificant damage to the cell walls of MR-1.

We also studied the electron transport system activity (ETSA) of MR-1 after EPS extraction at 30°, 38°, and 100°C for 30 min to evaluate the effects of heat treatment on respiratory metabolism (*26*). ETSA decreased by heating at 100°C, but MR-1 treated at 38°C showed very similar ETSA as those treated at 30°C (Fig. 4F). Further electrochemical measurements have also indicated that the heat treatment at 38°C did not induce a notable change of the redox protein expression and the activity of MR-1 (figs. S6 and S7). Together, these data strongly suggest that the observed voltammetric differences between MR-1 in the presence and absence of EPS are not caused by cell damage.

Hence, we conclude that mainly flavins and c-type cytochromes in EPS contribute to the DPV peaks and *i-t* current increment for MR-1 (fig. S5): (i) flavin DPV cannot be detected after EPS extraction but detected only in EPS extracts; (ii) after 48 hours of cultivation, most of the cell surface is covered by EPS, which separates c-type cytochromes from the electrode (most c-type cytochromes on the cell surface therefore cannot interact directly with the electrode) (Fig. 2B) ; (iii) the DPV peaks of the flavin/MtrC combination are only detected after EPS extraction; (iv) the presence of cytochromes and flavins is confirmed by UV-vis spectrometry; and (v) the direct presence of c-type cytochromes in EPS has been reported for the *Shewanella* strain (*27*).

Electrons are transported through EPS by hopping

Electron hopping and tunneling are core notions in long-range ET processes in biological systems (*28*). Direct tunneling gives 10 or 15 orders of magnitude current decrease over a 35-nm layer of polysaccharides (see Supplementary Discussion and table S1) and is excluded here. On the other hand, less than an order of magnitude current decrease is associated with hopping between closely spaced ET sites. These concepts are examined below and in the Supplementary Discussion. Electron "hopping" represents the EET processes in the presence of EPS, and we propose that EPS act as transient media for electron hopping as the prevailing pathway for natural microbial EET (Fig. 5).

Hopping requires a high density of ET sites, and the feasibility of ET by hopping across the membrane/EPS layer is examined below. The number of electroactive ET sites corresponds to the total formal charge Q_{formal} in the adlayer and can be determined from the DPV peak charge Q_{DPV}. However, Q_{DPV} is a differential quantity and not directly the formal charge, Q_{formal}, as in CV. The correlation between Q_{DPV} and Q_{formal} for reversible thin-layer DPV, and small DPV potential increments ΔE(V), is (cf. Supplementary Discussion)

$$Q_{DPV} = \pi \frac{k_0 \Delta E}{\nu} Q_{formal} \quad (1)$$

where k_0 (s^{-1}) is the standard electrochemical ET rate constant. Equation 1 enables obtaining the product $Q_{formal} \times k_0$. Using $k_0 = 0.026\ s^{-1}$ estimated from the CVs, fig. S3 gives the values of both Q_{DPV} and Q_{formal} of all the DPV peaks summarized in table S3. The Q_{DPV} values are in the range 1×10^{-9} to 10×10^{-9} C for MR-1, 1×10^{-8} to 2.5×10^{-8} C for EPS-depleted MR-1, and 1.5×10^{-9} to 7×10^{-9} C for isolated EPS, whereas Q_{formal} is in the range 3×10^{-8} to 40×10^{-8} C corresponding to 3×10^{-13} to 40×10^{-13} moles or 2×10^{11} to 25×10^{11} molecules. These numbers give the average total number of single-ET redox carriers over a 3-mm electrode surface. If these were evenly distributed over a 35-nm membrane/EPS layer on the electrode surface, that is, 0.245 nl of EPS, a molar concentration of 10^{-3} to 10^{-2} M would emerge or an average distance between the molecular redox sites of 5 to 10 nm. This value is subject to the reservation discussed in the Supplementary Discussion, and the concentration could be up to five times lower, within 10^{-4} to 10^{-3} M or about twice longer than the average intersite distance.

"Metallic conductivity" has been forwarded as an alternative ET mechanism (*2*). The experimental conditions by Lovley (*2*) are, however, quite different from the current study, in which an aqueous environment was used, in contrast to an ambient "dry" environment (*28*). The electrochemical signals are furthermore carried by cytochromes and flavins, of well-defined structure and redox potentials, and testify to localized electronic states. Band conductivity requires oxidation or reduction in other structural elements, such as aromatic side groups. These electrochemical signals are associated with high energies and were not detected in the present study, leaving hopping as the prevailing molecular mechanism, although tunneling is crucial in the individual "hops" (cf. below) (*29*).

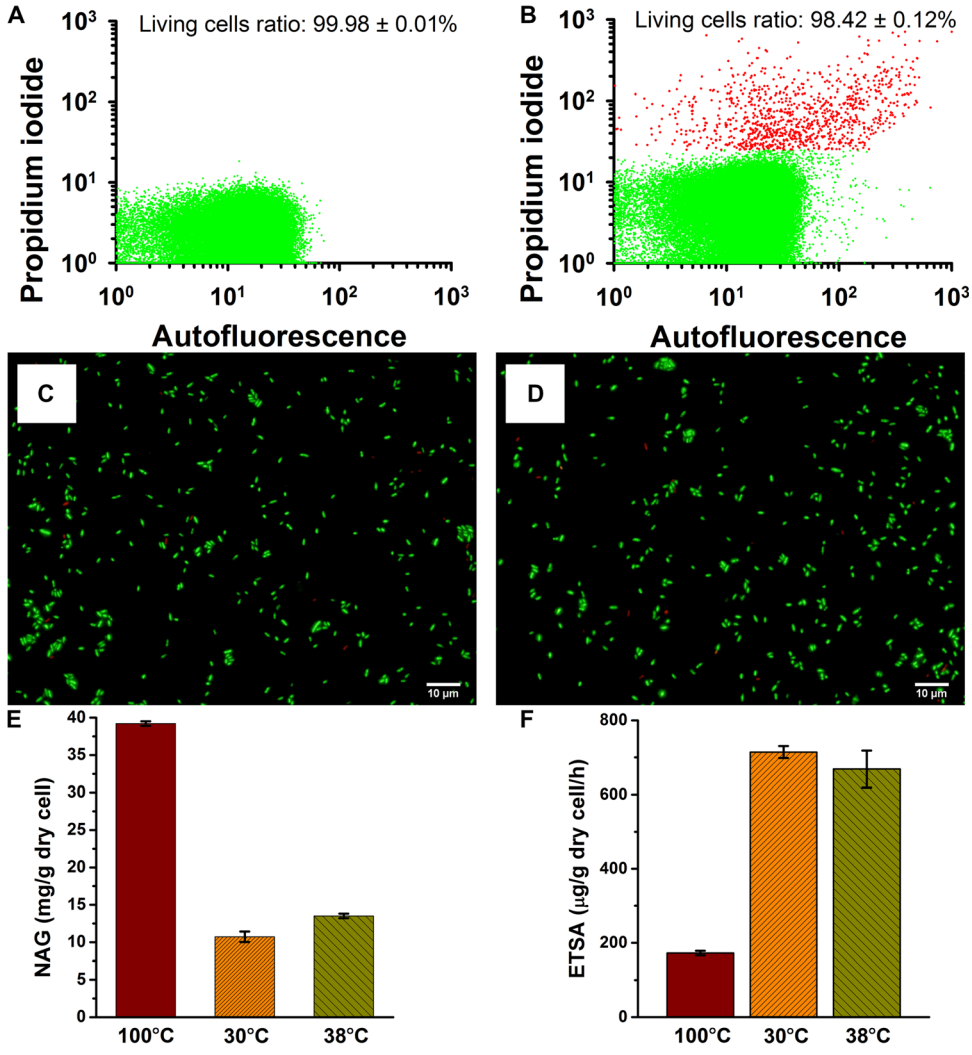

Fig. 4. Integrity tests on MR-1 cells. (**A** and **B**) Flow cytometry shows that EPS extraction only destroys insignificantly the MR-1 cells. (A) Flow cytometry of MR-1 cells treated at 30°C. (B) Flow cytometric analysis of MR-1 cells treated at 38°C for EPS extraction. Green and red spots are living and dead cells, respectively. (**C** and **D**) LIVE/DEAD staining of MR-1 cells shows similar ratios of live cells to total MR-1 cells in the presence (C) and absence (D) of EPS. (**E**) The concentration of NAG in EPS extracted at different temperatures. (**F**) The ETSA of MR-1 cells after EPS extraction at different temperatures. Samples in all experiments at different temperatures are heat-treated for 30 min.

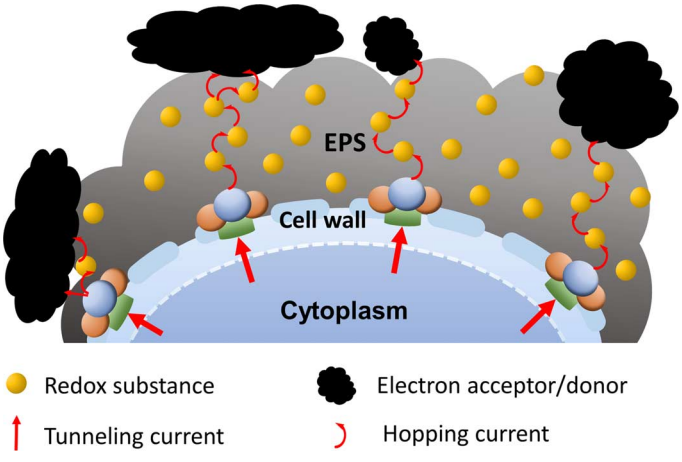

Fig. 5. Schematic of EPS as transient media for microbial EET by electron hopping.

Hopping implies ET between localized states and strong electronic-vibrational interactions with full vibrational relaxation, represented by rate constant W (s^{-1}) of the generic form

$$W = \kappa_0 \exp(-\beta\Delta R)\frac{\omega_{\text{eff}}}{2\pi}\exp\left[-\frac{(\lambda+\Delta G^0)^2}{4\lambda k_B T}\right];$$
$$\kappa = \kappa_0 \exp(-\beta\Delta R)(\kappa < 1) \quad (2)$$

where $\omega_{\text{eff}}/2\pi$ ($\approx 10^{12}$ s^{-1}) (*29*) is the effective vibrational frequency of the nuclear modes. The activation free energy is determined by the nuclear reorganization free energy λ and the reaction free energy (ΔG_0). k_B is Boltzmann's constant, T is the temperature, and κ is the electronic transmission coefficient. In the diabatic limit of weak interaction, κ is determined by the hop distance ΔR and the decay factor β ($Å^{-1}$). Here, κ_0 can be taken as unity. In the opposite, the adiabatic limit of strong interaction is $\kappa \to 1$. Analogous forms apply to the electrochemical rate constant (*29*).

Points to notice are as follows:

(1) Equation 2 represents the transition probability per unit time in a single hop and holds a nuclear activation factor and an electronic coupling (tunneling) factor. Tunneling is thus an integrated feature in hopping.

(2) Fast hopping requires small nuclear reorganization energy and weakly exothermic ET. Cytochromes and flavins accord with these requirements. Efficient hops must also be adiabatic or weakly diabatic, $\kappa \rightarrow 1$, that is, with close contact distance (*30*).

(3) The transition between hopping and band conduction is crudely determined by the condition $V_{DA}/\lambda \approx 1$, where V_{DA} is the electronic coupling between a donor and an acceptor. V_{DA}/λ is always smaller than unity for ET between localized states in disordered media, and hopping prevails in the present study.

(4) Hopping rate constants can be formally converted to conductivity (*28*, *31*), but electrochemical CVs are better described formally by notions of diffusion (*32*) in semi-infinite or confined space. The "diffusion coefficient," D, is then (*32*, *33*)

$$D = n \times W(\Delta R) \times P \times \Delta R^2 \quad (3)$$

where P is the probability that a vacant hopping site is available at the distance ΔR and n is a geometric factor.

Equations 2 and 3 offer a view of the feasibility of electrochemical hopping across the EPS layer. Taking $n = 1$ and a high density of hopping sites, $P \rightarrow 1$, the diffusion (that is, hopping) length, ℓ within the time t is $1 \approx \sqrt{Dt}$. For diffusion to reach ℓ within the time t, the condition

$$W \geq \frac{1}{t}\left(\frac{1}{\Delta R}\right)^2 \quad (4)$$

must therefore apply. This condition is less restrictive. If t is taken for the time of a DPV sweep, for example, 100 s, $\ell = 35$ nm, and $\Delta R = 1$ nm, Eq. 4 gives $W \geq 10\ s^{-1}$ for hopping to be efficient. For close to contact distance of the hopping sites, $\kappa \rightarrow 1$, and approximately thermoneutral hops, Eq. 2 reduces to

$$W \rightarrow \frac{\omega_{eff}}{2\pi} \exp\left(-\frac{\lambda}{4k_B T}\right) \quad (5)$$

The condition $W \geq 10\ s^{-1}$ then leaves a wide margin, and diffusion across the membrane within 100 s is feasible for reorganization free energies up to 250 kJ, corresponding to an activation free energy of about 60 kJ. If the ET distance is 2 nm, corresponding to a decrease of the transmission coefficient from unity to 5×10^{-5}, diffusion or hopping is still feasible, provided that the activation free energy is now less than about 40 kJ, but the following is to be noted. Cytochromes are large molecules. With a decaheme composition, the molecular diameter would be about 5 to 10 nm (*34*). However, the hopping centers are the individual heme groups inside the decaheme cyt molecules, with an average intersite distance of only 1 to 2 nm, in a wire-like close-distance structural organization, instead of 5 to 10 nm estimated from DPV. Efficient hopping must therefore imply that the electrochemically active decaheme cyt centers are spatially confined either within a thinner layer than the full 35-nm pili volume or in "wires" vertical to the electrode surface. "Vehicular" diffusion of mobile flavin carriers across the EPS can therefore also be involved.

Voltammetry of Gram-positive *Bacillus* sp. WS-XY1 and yeast *Ps* supports the hypothesis

Compared to Gram-negative bacteria, Gram-positive bacteria and yeast have different cell wall structures. These are a thicker peptidoglycan layer in Gram-positive bacteria and a thicker glucan layer in yeast. These differences in membrane structure may induce changes of the EET pathways in Gram-positive bacteria and yeast. Most electrochemically active microorganisms are Gram-negative bacteria (*35*), but some Gram-positive bacteria and yeasts, such as WS-XY1 and *Ps* (*19*), are also electrochemically active. The two strains WS-XY1 and *Ps* were therefore also chosen to address the role of EPS in the EET processes of Gram-positive bacteria and yeast, respectively (figs. S8 to S10). Two anodic and two cathodic DPV peaks of WS-XY1 and *Ps* were detected both for control groups and EPS-depleted groups (Fig. 6 and fig. S11).

The DPV peaks around −0.4 V are ascribed to flavins (*19*). Notably, these peaks increase significantly after EPS extraction, whereas the flavin peaks disappeared in MR-1 after EPS depletion. Both these peaks are also detected in the EPS extract (Fig. 6, C and D). These results suggest that voltammetric flavin peaks for normal strains (that is, the control group) are contributed by flavins in two states, that is, in EPS and combined with cell walls. EPS extraction enhances the cell peak heights around −0.1 V, and peaks at similar potentials were detected in extracted EPS (Fig. 6). These results indicate that EPS from WS-XY1 and *Ps* are electrochemically active and play an important role as transient media for microbial EET.

CONCLUSION

Because of the EPS' strong redox ability and 3D structure, electron transport between microbial cells and extracellular electron acceptors/donors, whether via pili/nanowires, membrane-bound proteins, or electron shuttles, must therefore take the effect of EPS into account. Considering the spatial distances, membrane-bound cytochromes are not able to directly transfer electrons to extracellular electron acceptors when a thick layer of EPS covers the cell surface. It is also important to understand the influence of the redox reactions of EPS in conductive nanowires for EET and if some electrons are transported from the surface of conductive nanowires into the EPS (not extracellular electron acceptors) via redox reactions. Results from the three strains show that EPS attenuates direct EET, although the strains remain electrochemically active (Fig. 3, A and B, fig. S5, and table S2). When EPS-depleted cells are exposed to harsh conditions, proteins on the cell surface are easily inactivated, or the cells even killed and EET lost. EPS help cells to attach on solid minerals or other electron acceptors/donors and shorten the gap between microorganisms and solid surfaces. This not only facilitates EET but also saves the energy used to reach the acceptors/donors (*36*). We suggest that these strains achieve a successful balance between EET, self-protection, and other natural EPS functions.

Indirect EET is another major microbial EET pathway (*8*) that may benefit from the presence of EPS, because EPS help microorganisms maintain a high concentration of electron shuttles in the gap between cells and electron acceptors/donors. Unbound flavins as electron mediators have to diffuse within the EPS layer, which shows different fluid mechanics compared with those in bulk solution. Moreover, it is not possible to detect the bound flavin-cytochrome interaction until this EPS layer is removed.

In brief, the current work shows that EPS store electrochemically active substances (such as flavins and c-type cytochromes), which act

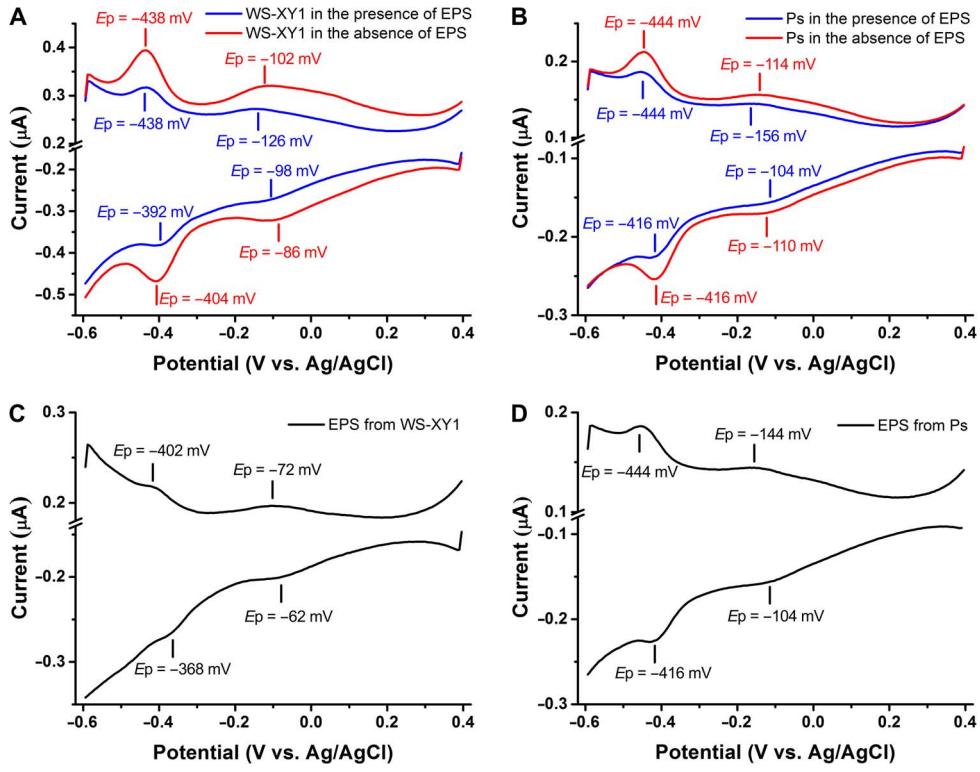

Fig. 6. DPV of cells and EPS of WS-XY1 and *Ps*. (**A** and **B**) DPV of WS-XY1 (A) and *Ps* (B) cells in the presence and absence of EPS. (**C** and **D**) DPV of EPS extract from WS-XY1 (C) and *Ps* (D) strains.

as electron transit media. This enables EPS-enveloped cells to transport extracellularly electrons to acceptors or from donors by EET, where electron hopping is the most likely molecular mechanism for electrochemical ET through EPS.

MATERIALS AND METHODS

Bacterial strains and growth conditions

Strains of MR-1, WS-XY1, and *Ps* were grown statically at 30°C for 48 hours. Luria-Bertani broth medium was used to culture MR-1, Luria-Bertani broth medium without yeast extract was used to culture WS-XY1, and peptone dextrose medium (2% peptone, 2% dextrose) was used to culture strain *Ps* (*19*). All media were adjusted to an initial pH of 7.0.

EPS extraction

Heat treatment can remove EPS by enhancing the molecular, protein, and membrane dynamics, and hence accelerating the EPS dissolution in extract solution (*13*), and our previous study has shown that heat treatment is an efficient method for EPS extraction (*20*). The cells were harvested by centrifugation (5000*g*, 10 min, 4°C) and washed twice with 0.9% NaCl (w/v) solution. Washed cell pellets were resuspended in 0.9% NaCl (w/v) solution and heated in a water bath at different temperatures (optimally, 38°C for MR-1, 45°C for WS-XY1, and 55°C for *Ps*) for 30 min. Cell suspensions were centrifuged once again (5000*g*, 10 min, 4°C), and cell pellets were collected for electrochemical measurements and morphology analysis. The supernatant was filtered through a 0.22-μm filter to remove unsettled cells. The filtrate (that is, EPS) was stored at 4°C for later chemical analysis. Cells treated at 30°C were used as control groups.

Electrochemical measurements

All electrochemical data were recorded using an Autolab electrochemical workstation with a three-electrode chamber containing a glassy carbon electrode (3-mm diameter), a platinum-wire counter electrode, and an Ag/AgCl reference electrode with saturated KCl (potential versus the normal hydrogen electrode, +198 mV). All potentials refer to the Ag/AgCl reference electrode. In all electrochemical measurements, cell pellets treated at different temperatures were resuspended in phosphate buffer (50 mM, pH 7.0). Cell suspension (10 μl) (containing about 1×10^7 cells) was then drop-casted on the glassy carbon electrode and mixed with 1 μl of 1% Nafion aqueous solution to form a layer of biofilm. Phosphate buffer solution (50 mM, pH 7.0) was used as electrolyte. All experiments were conducted under a nitrogen atmosphere. The parameters were as follows: for CV: resting time, 8 s; scan rate, 10 mV/s; $E_i = -0.6$ V; and $E_f = 0.4$ V; for DPV: $E_i = -0.6$ V; $E_f = 0.4$ V; amplitude, 60 mV; pulse width, 200 ms; and potential increment, 6 mV; for *i-t* chronoamperometry: $E = 0.3$ V.

Flow cytometry and morphology measurements

To evaluate the cell viability after EPS extraction, the cells were fluorescence-stained with propidium iodide and measured by flow cytometry (Quanta SC, Beckman Coulter) after 30 min of heat treatment. About 10,000 cells were analyzed for each sample. After heat treatment, the cells were also stained with the LIVE/DEAD *Bac*Light Bacterial Viability Kit (Molecular Probes, Eugene) containing the two fluorescent dyes: SYTO 9 and propidium iodide. The staining procedure was conducted according to the manufacturer's instruction. The cells stained with the two fluorescent dyes were observed by inverted fluorescence microscopy (IX71, Olympus). AFM (AFM5500, Agilent) in contact mode was used to compare the morphology of MR-1 cells in the presence and absence of EPS. The cells

were drop-casted on freshly cleaned platinum sheets and dried in air for at least 4 hours.

Chemical analysis

The ETSA was determined according to the protocol described by Relexans (*37*) with some modifications. 2,3,5-Triphenyltetrazolium chloride (TTC) was used as the artificial electron acceptor, with acetone as extractant. A mixture of 1 ml of cell suspension and 2 ml of 0.4% TTC solution was incubated in a rotary incubator (150 rpm) at 30°C for 30 min. The reaction mixture was then centrifuged (4000*g*, 5 min, 25°C), and the supernatant was discarded. The triphenyl formazan produced was extracted with 5 ml of acetone, and the concentration was recorded at 485 nm by UV-vis spectroscopy. The concentration of NAG in the EPS extract was determined according to the modified Schales' procedure (*38*). A cell suspension of 1.5 and 2 ml of potassium hexacyanoferrate(III) reagent [0.5 g of potassium hexacyanoferrate(III) in 1 liter of 0.5 M Na_2CO_3] was mixed and heated in a boiling water bath for 15 min. The optical density at 420 nm was read after cooling. UV-vis measurements were conducted using an Agilent 8354 instrument. NaCl (0.9% w/v) was used as a blank, and 10 ml EPS extract originating from 25 ml of MR-1 culture was recorded in the wavelength range 190 to 1190 nm. Spectra of pure riboflavin (Sigma-Aldrich) were also recorded.

Size determination

The size distribution of the cell suspension was determined by a laser particle size analyzer (MS2000, Malvern Instruments). According to the manual from the manufacturer, the size analyzer results provide the equivalent sphere diameter with the same volume of the measured cell. From AFM morphology observations, most MR-1 cells are rod-shaped with length/width ratios of about 3. To simplify the calculation of cell size, a cell was taken as equivalent to a cylinder with a length/radius ratio of 6. We then determined the length and radius of the cylinder-shaped cell using the following equations

$$V_{es} = \frac{1}{6}\pi \cdot d_{es}^3 \quad (6)$$

$$V_{cell} = \pi \cdot r_{cell}^2 \cdot l = 6\pi \cdot r_{cell}^3 \quad (7)$$

$$r_{cell} = \sqrt[3]{\frac{1}{36}} \cdot d \approx 0.3d \quad (8)$$

where V_{es} is the volume of the equivalent sphere, d_{es} is the diameter of the equivalent sphere, V_{cell} is the volume of the measured cell equal to V_{es}, r_{cell} is the radius, and l is the length of the cell.

SUPPLEMENTARY MATERIALS

Supplementary material for this article is available at http://advances.sciencemag.org/cgi/content/full/3/7/e1700623/DC1

Supplementary Discussion

fig. S1. 3D AFM images of *S. oneidensis* MR-1 cells.

fig. S2. Yields of different EPS components from MR-1.

fig. S3. CV of *S. oneidensis* MR-1 cells in the presence (blue line) and absence (red line) of EPS.

fig. S4. UV-vis spectra of EPS from MR-1.

fig. S5. Chronoamperometry *i-t* test on MR-1 cells.

fig. S6. DPV curves for MR-1 cell pellets treated at 30° and 38°C.

fig. S7. DPV curves for MR-1 cell culture treated at 30° and 38°C.

fig. S8. Effect of different heating temperatures on microbial viability evaluated by flow cytometry.

fig. S9. Yields of different EPS components from strains WS-XY1 and *Ps*.

fig. S10. Live/Dead staining of WS-XY1 and *Ps* cells after heating treatments.

fig. S11. CV of pure and EPS-depleted cells of WS-XY1 and *Ps*.

table S1. Size determination of MR-1 cells using a laser particle size analyzer.

table S2. Amperometric *i-t* test for MR-1 cells.

table S3. Charge calculation based on DPV shown in Fig. 3.

References (*39*–*42*)

REFERENCES AND NOTES

1. M. E. Hernandez, D. K. Newman, Extracellular electron transfer. *Cell. Mol. Life Sci.* **58**, 1562–1571 (2001).
2. D. R. Lovley, Electromicrobiology. *Annu. Rev. Microbiol.* **66**, 391–409 (2012).
3. B. E. Logan, Exoelectrogenic bacteria that power microbial fuel cells. *Nat. Rev. Microbiol.* **7**, 375–381 (2009).
4. D. R. Lovley, Bug juice: Harvesting electricity with microorganisms. *Nat. Rev. Microbiol.* **4**, 497–508 (2006).
5. S. E. McGlynn, G. L. Chadwick, C. P. Kempes, V. J. Orphan, Single cell activity reveals direct electron transfer in methanotrophic consortia. *Nature* **526**, 531–535 (2015).
6. G. Wegener, V. Krukenberg, D. Riedel, H. E. Tegetmeyer, A. Boetius, Intercellular wiring enables electron transfer between methanotrophic archaea and bacteria. *Nature* **526**, 587–590 (2015).
7. F. Zhao, R. C. T. Slade, J. R. Varcoe, Techniques for the study and development of microbial fuel cells: An electrochemical perspective. *Chem. Soc. Rev.* **38**, 1926–1939 (2009).
8. E. Marsili, D. B. Baron, I. D. Shikhare, D. Coursolle, J. A. Gralnick, D. R. Bond, *Shewanella* secretes flavins that mediate extracellular electron transfer. *Proc. Natl. Acad. Sci. U.S.A.* **105**, 3968–3973 (2008).
9. R. S. Hartshorne, C. L. Reardon, D. Ross, J. Nuester, T. A. Clarke, A. J. Gates, P. C. Mills, J. K. Fredrickson, J. M. Zachara, L. Shi, A. S. Beliaev, M. J. Marshall, M. Tien, S. Brantley, J. N. Butt, D. J. Richardson, Characterization of an electron conduit between bacteria and the extracellular environment. *Proc. Natl. Acad. Sci. U.S.A.* **106**, 22169–22174 (2009).
10. M. Y. El-Naggar, G. Wanger, K. M. Leung, T. D. Yuzvinsky, G. Southam, J. Yang, W. M. Lau, K. H. Nealson, Y. A. Gorby, Electrical transport along bacterial nanowires from *Shewanella oneidensis* MR-1. *Proc. Natl. Acad. Sci. U.S.A.* **107**, 18127–18131 (2010).
11. H.-C. Flemming, J. Wingender, U. Szewzyk, P. Steinberg, S. A. Rice, S. Kjelleberg, Biofilms: An emergent form of bacterial life. *Nat. Rev. Microbiol.* **14**, 563–575 (2016).
12. H.-C. Flemming, T. R. Neu, D. J. Wozniak, The EPS matrix: The "house of biofilm cells". *J. Bacteriol.* **189**, 7945–7947 (2007).
13. G.-P. Sheng, H.-Q. Yu, X.-Y. Li, Extracellular polymeric substances (EPS) of microbial aggregates in biological wastewater treatment systems: A review. *Biotechnol. Adv.* **28**, 882–894 (2010).
14. B. C. van der Aa, Y. F. Dufrêne, In situ characterization of bacterial extracellular polymeric substances by AFM. *Colloids Surf. B Biointerfaces* **23**, 173–182 (2002).
15. A. C. Dohnalkova, M. J. Marshall, B. W. Arey, K. H. Williams, E. C. Buck, J. K. Fredrickson, Imaging hydrated microbial extracellular polymers: Comparative analysis by electron microscopy. *Appl. Environ. Microbiol.* **77**, 1254–1262 (2011).
16. A. P. Borole, G. Reguera, B. Ringeisen, Z.-W. Wang, Y. Feng, B. H. Kim, Electroactive biofilms: Current status and future research needs. *Energ. Environ. Sci.* **4**, 4813–4834 (2011).
17. M. J. Marshall, A. S. Beliaev, A. C. Dohnalkova, D. W. Kennedy, L. Shi, Z. Wang, M. I. Boyanov, B. Lai, K. M. Kemner, J. S. McLean, S. B. Reed, D. E. Culley, V. L. Bailey, C. J. Simonson, D. A. Saffarini, M. F. Romine, J. M. Zachara, J. K. Fredrickson, *c*-Type cytochrome-dependent formation of U(IV) nanoparticles by Shewanella oneidensis. *PLOS Biol.* **4**, e268 (2006).
18. S.-W. Li, G.-P. Sheng, Y.-Y. Cheng, H.-Q. Yu, Redox properties of extracellular polymeric substances (EPS) from electroactive bacteria. *Sci. Rep.* **6**, 39098 (2016).
19. S. Wu, Y. Xiao, L. Wang, Y. Zheng, K. Chang, Z. Zheng, Z. Yang, J. R. Varcoe, F. Zhao, Extracellular electron transfer mediated by flavins in Gram-positive *Bacillus* sp. WS-XY1 and yeast *Pichia stipitis*. *Electrochim. Acta* **146**, 564–567 (2014).
20. Y.-F. Dai, Y. Xiao, E.-H. Zhang, L.-D. Liu, L. Qiu, L.-X. You, G. Dummi Mahadevan, B.-L. Chen, F. Zhao, Effective methods for extracting extracellular polymeric substances from *Shewanella oneidensis* MR-1. *Water Sci. Technol.* **74**, 2987–2996 (2016).
21. A. Okamoto, K. Hashimoto, K. H. Nealson, R. Nakamura, Rate enhancement of bacterial extracellular electron transport involves bound flavin semiquinones. *Proc. Natl. Acad. Sci. U.S.A.* **110**, 7856–7861 (2013).
22. A. A. Carmona-Martinez, F. Harnisch, L. A. Fitzgerald, J. C. Biffinger, B. R. Ringeisen, U. Schröder, Cyclic voltammetric analysis of the electron transfer of *Shewanella oneidensis* MR-1 and nanofilament and cytochrome knock-out mutants. *Bioelectrochemistry* **81**, 74–80 (2011).
23. P. S. Jensen, Q. Chi, F. B. Grumsen, J. M. Abad, A. Horsewell, D. J. Schiffrin, J. Ulstrup, Gold nanoparticle assisted assembly of a heme protein for enhancement of long-range interfacial electron transfer. *J. Phys. Chem. C* **111**, 6124–6132 (2007).

24. L. Boulos, M. Prévost, B. Barbeau, J. Coallier, R. Desjardins, LIVE/DEAD®*Bac*Light™: Application of a new rapid staining method for direct enumeration of viable and total bacteria in drinking water. *J. Microbiol. Methods* **37**, 77–86 (1999).
25. T. Nagata, B. Meon, D. L. Kirchman, Microbial degradation of peptidoglycan in seawater. *Limnol. Oceanogr.* **48**, 745–754 (2003).
26. A. Broberg, A modified method for studies of electron transport system activity in freshwater sediments. *Hydrobiologia* **120**, 181–187 (1985).
27. B. Cao, L. Shi, R. N. Brown, Y. Xiong, J. K. Fredrickson, M. F. Romine, M. J. Marshall, M. S. Lipton, H. Beyenal, Extracellular polymeric substances from *Shewanella* sp. HRCR-1 biofilms: Characterization by infrared spectroscopy and proteomics. *Environ. Microbiol.* **13**, 1018–1031 (2011).
28. N. F. Polizzi, S. S. Skourtis, D. N. Beratan, Physical constraints on charge transport through bacterial nanowires. *Faraday Discuss.* **155**, 43–62 (2012).
29. A. Kuznetsov, J. Ulstrup, *Electron Transfer in Chemistry and Biology: An Introduction to the Theory* (John Wiley & Sons Inc., 1998).
30. J. R. Winkler, H. B. Gray, Long-range electron tunneling. *J. Am. Chem. Soc.* **136**, 2930–2939 (2014).
31. S. Pirbadian, M. Y. El-Naggar, Multistep hopping and extracellular charge transfer in microbial redox chains. *Phys. Chem. Chem. Phys.* **14**, 13802–13808 (2012).
32. D. N. Blauch, J. M. Saveant, Dynamics of electron hopping in assemblies of redox centers. Percolation and diffusion. *J. Am. Chem. Soc.* **114**, 3323–3332 (1992).
33. A. A. Kornyshev, A. M. Kuznetsov, E. Spohr, J. Ulstrup, Kinetics of proton transport in water. *J. Phys. Chem. B* **107**, 3351–3366 (2003).
34. A. Messerschmidt, *Handbook of metalloproteins* (Wiley, 2001).
35. Y. Xiao, S. Wu, Z.-H. Yang, Y. Zheng, F. Zhao, Isolation and identification of electrochemically active microorganisms. *Prog. Chem.* **25**, 1771–1780 (2013).
36. H. W. Harris, M. Y. El-Naggar, O. Bretschger, M. J. Ward, M. F. Romine, A. Y. Obraztsova, K. H. Nealson, Electrokinesis is a microbial behavior that requires extracellular electron transport. *Proc. Natl. Acad. Sci. U.S.A.* **107**, 326–331 (2010).
37. J. C. Relexans, Measurement of the respiratory electron transport system (ETS) activity in marine sediments: State-of-the-art and interpretation. I. Methodology and review of literature data. *Mar. Ecol. Prog. Ser.* **136**, 277–287 (1996).
38. T. Imoto, K. Yagishita, A simple activity measurement of lysozyme. *Agric. Biol. Chem.* **35**, 1154–1156 (1971).
39. K. Aoki, K. Tokuda, H. Matsuda, Theory of differential pulse voltammetry at stationary planar electrodes. *J. Electroanal. Chem.* **175**, 1–13 (1984).
40. J. L. Melville, R. G. Compton, The simulation of differential pulse voltammetry. *Electroanalysis* **13**, 123–130 (2001).
41. A. L. Y. Lau, A. T. Hubbard, Study of the kinetics of electrochemical reactions by thin-layer voltammetry: III. Electroreduction of the chloride complexes of platinum(II) and (IV). *J. Electroanal. Chem.* **24**, 237–249 (1970).
42. E. Laviron, L. Roullier, C. Degrand, A multilayer model for the study of space distributed redox modified electrodes: Part II. Theory and application of linear potential sweep voltammetry for a simple reaction. *J. Electroanal. Chem.* **112**, 11–23 (1980).

Acknowledgments: We thank H. B. Gray (California Institute of Technology) for the comments and suggestions on this work. **Funding:** This study was supported by grants from the National Natural Science Foundation of China (51478451, 51208490, and 21322703), the Knowledge Innovation Program of the Chinese Academy of Sciences (IUEQN201306), the Carlsberg Foundation (CF15-0164), the Otto Mønsted Foundation, and the National Key Scientific Instrument and Equipment Development Project (2013YQ17058508). **Author contributions:** Y.X. and F.Z. conceived and designed the study. Y.X., E.Z., and Y.D. acquired the data. Y.X., E.Z., J.Z., J.U., and F.Z. analyzed and interpreted the data. Y.X., J.Z., and J.U. performed the theoretical calculation. Y.X., E.Z., J.Z., Z.Y., H.E.M.C., J.U., and F.Z. drafted or revised the article. All authors approved the final manuscript. **Competing interests:** The authors declare that they have no competing interests. **Data and materials availability:** All data needed to evaluate the conclusions in the paper are present in the paper and/or the Supplementary Materials. Additional data related to this paper may be requested from the authors.

Submitted 1 March 2017
Accepted 18 May 2017
Published 5 July 2017
10.1126/sciadv.1700623

Citation: Y. Xiao, E. Zhang, J. Zhang, Y. Dai, Z. Yang, H. E. M. Christensen, J. Ulstrup, F. Zhao, Extracellular polymeric substances are transient media for microbial extracellular electron transfer. *Sci. Adv.* **3**, e1700623 (2017).